Available online at www.sciencedirect.com
ScienceDirect
International Journal of Thermal Sciences 47 (2008) 1195–1203
International Journal of Thermal Sciences
www.elsevier.com/locate/ijts

The experimental investigation on thermal performance of a flat two-phase thermosyphon

Ming Zhang, Zhongliang Liu *, Guoyuan Ma

Key Laboratory of Enhanced Heat Transfer and Energy Conservation, Ministry of Education and Key Laboratory of Heat Transfer and Energy Conversion, Beijing Education Commission, College of Environmental and Energy Engineering, Beijing University of Technology, Beijing 100022, PR China

Received 5 April 2007; received in revised form 9 October 2007; accepted 9 October 2007

Available online 5 March 2008

Abstract

Electronics cooling has become a key factor for improving the performance of electronic devices. An effective thermal spreader can achieve a more uniform heat flux distribution and thus increase heat dissipation in heat sinks. Two-phase thermosyphon is highly effective thermal spreader. In order to observe boiling and condensation phenomena, a transparent two-phase thermosyphon was prepared for observation and study. The characteristics of phase change heat transfer were experimentally investigated. The performance of the two-phase thermosyphon with different working fluids was measured for different heat fluxes. The experimental results show that it has the ability to level temperature and produces a very uniform temperature distribution in the condensation surface. The impairment of cooling condition on the external side of the condensation plate worsens the performance of the two-phase thermosyphon. Throughout the tested heat flux range in our experiment, the two-phase thermosyphon with water as working fluid has a better performance than that with ethanol as working fluid. We also studied the ability of the grooved evaporation surface to increase boiling heat transfer. Our experiments prove that the two-phase thermosyphon with a grooved evaporation surface has a much better performance due to the increased heat transfer at the evaporation surface. By comparing the thermal resistance of a solid copper plate to that of the two-phase thermosyphon, it is suggested that the critical heat flux condition should be maintained if two-phase thermosyphon is to be used as efficient thermal spreaders for electronics cooling.

Keywords: Two-phase thermosyphon; Electronics cooling; Grooved surface; Thermal resistance

1. Introduction

The technology of electronics cooling has become a key factor for further improvement of the performance of various electronic devices, especially microcomputers. Electronic devices usually dissipate very high heat fluxes. In order to dissipate heat efficiently, the heat sink is generally much larger than the heat source. So a spreader is usually placed between the heat source and the heat sink to level the heat flux distribution. The spreading resistance from the heat source to the heat sink is one major component of the total thermal resistance of cooling devices. The traditional spreader is a solid copper plate. Obviously the spreading resistance of this kind of spreader can be reduced by increasing plate thickness or improving the thermal conductivity of the plate. But materials with high thermal conductivity are usually quite expensive. An increase in plate thickness will also increase the weight of the spreader. So the performance of the traditional solid copper plate spreader is limited, especially at the large area of heat sink base and heating power.

Two-phase thermosyphon can achieve more uniform heat flux distribution, that is, by means of them a more uniform heat flux distribution can be obtained. These devices have a very high thermal conductance. A two-phase thermosyphon spreader is a kind of thermosyphon with special arrangement. Compared to the conventional thermosyphon, the evaporator and condenser sections are the opposite sides of it. The vapor channel is a very narrow space between the evaporation and the condensation surfaces. The working fluid boils at the evaporation surface and the generated vapor flows to and condensates on the condensation surface. In this way the heat can be trans-

* Corresponding author. Tel.: +86 10 67391917/67392566; fax: +86 10 67391983.

E-mail address: liuzhl@bjut.edu.cn (Z. Liu).

1290-0729/$ – see front matter
doi:10.1016/j.ijthermalsci.2007.10.004

Nomenclature

R_s	spreading resistance of solid copper plate	K/W
R_f	spreading resistance of two-phase thermosyphon	K/W
R_0	external resistance	K/W
Q	heating power	W
q	heating heat flux	W/m^2
T_{max}	maximal temperature of spreader	K
T_c	center temperature of condensation surface	K
T_e	center temperature of evaporation surface	K
T_r	room temperature	K
A_p	plate area	m^2
A_s	heat source area	m^2
k	thermal conductivity	W/(m K)
t	plate thickness	m
d	diameter of the heat source	m
D	diameter of the thermal spreader	m
$\overline{T}_{top}$	average temperature of top surface	K

ferred from the evaporator to the condenser. It is called "vapor chamber" or "flat plate heat pipe" in some other papers. By using a two-phase thermosyphon a nearly isothermal cooling surface can be obtained. A uniform temperature and thus a uniform heat flux distribution on the cooling surface also means a more effective heat dissipation from electronic devices, according to heat transfer theory.

McCreery [1] presented the design, construction and experimental results of a novel heat pipe. The apparatus is designed to enable the visual and photographic study of liquid flow and vapor formation within a flat heat pipe. Vafai and Wang [2] investigated the operation and overall performance of an asymmetrical rectangular flat plate heat pipe. Avenas et al. [3,4] carried out an analysis of the thermal resistance of a flat plate heat pipe. They compared the sintered wick with the grooved wick. Yasushi et al. [5] carried out a numerical analysis of a flat plate heat pipe with wick sheets and a wick column. From the numerical results, the capillary pressure head necessary for the working fluid to circulate is estimated and the temperature drop inside the vapor chamber is determined. Experimental research was also carried out. S.-W. Chen et al. [6] performed the experimental investigation and visualization of capillary and boiling limits of micro-grooves. Most of the previous work mainly paid attention to the performance of a two-phase thermosyphon for in different heat fluxes. The influence of the cooling condition on the condensation plate to the performance was not considered. Especially its inner pressure for different working fluids is not reported. The micro-grooves can enhance the performance of a two-phase thermosyphon, so it is essential to perform the experimental investigation of it with grooved structure. The two-phase thermosyphon spreader should be applied when a large base section of heat sink and a high heating power are involved. The critical heat flux condition which should be maintained to use it as an efficient thermal spreader is not studied in the previous work.

In order to study the thermal performance characteristics of a two-phase thermosyphon, we manufactured a transparent one for an observation study. There is no capillary structure between the evaporation and condensation surfaces, so that we can observe the phase change phenomena in it. The effects of power input, convection conditions and different working fluids on the performance of the two-phase thermosyphon were studied. The research was also carried out on the effect of grooved surface on increasing boiling heat transfer. By comparing the thermal resistance of a solid copper plate to that of the two-phase thermosyphon, it is suggested that the critical heat flux condition should be maintained to use it as an efficient thermal.spreader for electronics cooling.

2. Experimental setup and procedures

The apparatus used in this study include a blower, a data acquisition/switch unit, T-type thermocouples, an anemoscope, a transformer, a heating unit and a PC. Fig. 1 shows an outline of the experimental arrangement. To cool the two-phase thermosyphon, air is blown vertically onto its cooling surface. The air velocity is measured by the anemoscope. The heating heat flux is supplied by the heating unit. Adjusting the output voltage of the transformer can change the input power of the heating unit. Temperatures are measured by T-type thermocouples and collected through a data acquisition system. Fig. 2 shows the structure of the heating unit. The heating unit is a copper rod with four electrical rod heaters.

The rod diameter at the base is 60 mm and at the upper part the diameter is reduced to 30 mm to obtain a high enough heating heat flux for the two-phase thermosyphon. The copper rod is insulated and small insulating cushions are placed between the copper rod and the supporting framework to reduce heat losses. In order to reduce the contact resistance between the heating unit and the two-phase thermosyphon, high conductivity grease was applied to their contact surface. Tightening screws were

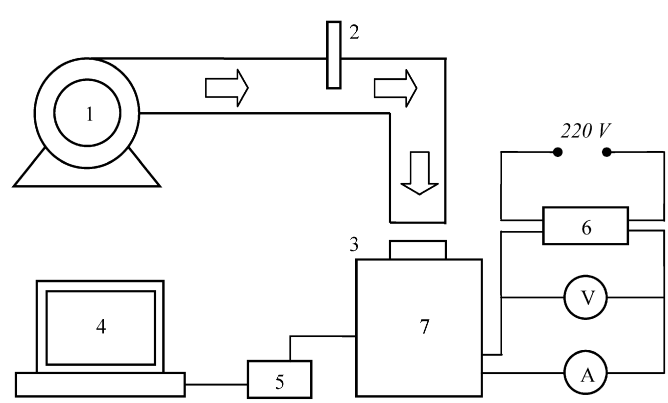

Fig. 1. Experimental system: 1, blower; 2, anemoscope; 3, flat plate heat pipe; 4, PC; 5, data acquisition/switch unit; 6, transformer; 7, heating unit.

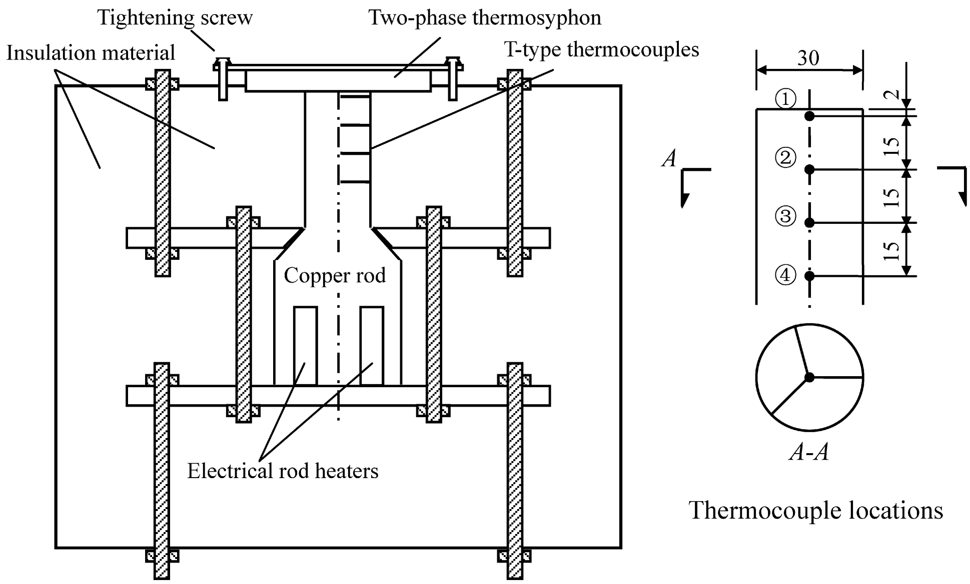

Fig. 2. Heating unit.

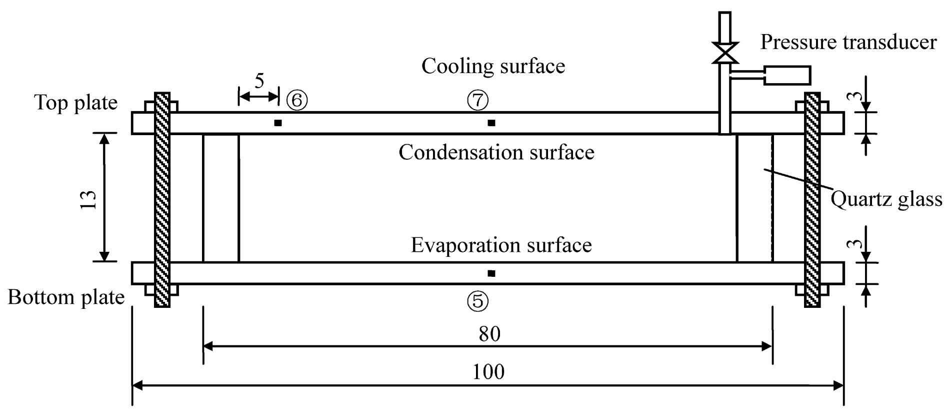

Fig. 3. Transparent two-phase thermosyphon.

also used to improve the contact between the two-phase thermosyphon and the heating unit. Points ① to ④ are the locations of the thermocouples used to measure the temperature distribution in the copper rod. There are 12 thermocouples are inserted in the copper rod to measure the temperature distribution in it. Three thermocouples are used to measure the temperature at each point. The locations of the thermocouples are shown in Fig. 2. Then the temperatures of points ① to ④ are the average of temperature values of three thermocouples. The insertion holes the thermocouples are 15 mm in depth and 1 mm in diameter. The 4 points at the axes of copper rod are located at 2, 17, 32 and 47 mm from the top surface of the copper rod, respectively. The steady state temperature distribution along the axial direction is thus obtained and thereafter used to calculate the temperature gradient.

Fig. 3 shows the structure of the transparent two-phase thermosyphon for observation study. In order to measure the temperature distribution of the evaporation and the condensation surfaces, 3 small holes were drilled into the bottom and top plates in order to insert 3 thermocouples. The locations of these 3 thermocouples (⑤, ⑥ and ⑦) are the center of the evaporation surface, a point 5 mm away from the edge of the condensation surface and the center of condensation surface.

The measure equipments in our experiment include anemoscope, pressure transducer and thermocouples. The uncertainties of the experimental results mainly depend on the precisions of these equipments. The precision of anemoscope is 5% and the precision of pressure transducer is 0.25% which had been determined by producers. Before experiment, all of the thermocouples have been measured with standard thermometer. After the calibration of thermocouples, the precision of thermocouple is 0.2%. In our experiment, we inserted these thermocouples into the small holes to measure the temperatures. The measure errors are caused by the contact thermal resistance. To reduce contact resistance and temperature measurement errors, high conductivity grease was applied into these holes. In our experimental rig, the heating power of heating surface is not equal to the heating power of electrical rod heaters in heating unit. A part of heat will be dissipated from the walls of the heating unit, though we have placed small insulating cushions between the copper rod and the supporting framework to reduce heat losses. Therefore, we use 12 thermocouples to

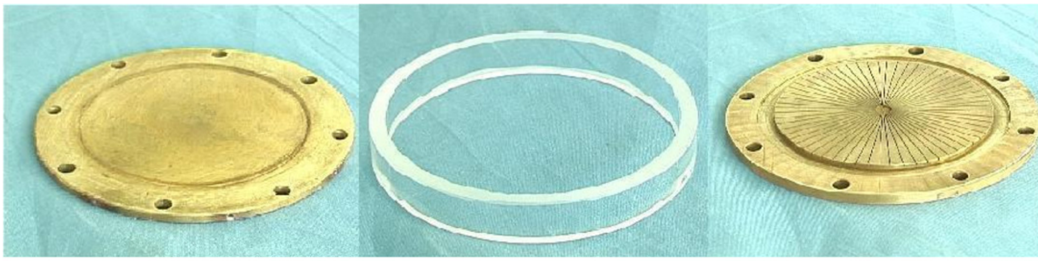

Fig. 4. Two-phase thermosyphon for observation study.

measure the temperatures of 4 points on the axis of copper rod. Every three thermocouples measure the temperature at one point to reduce the measure error. Then the heat flux of the heating unit is deduced from Fourier's law of heat conduction.

The side wall of the transparent two-phase thermosyphon is made of quartz glass. Its height, diameter and thickness are 13, 80 and 5 mm, respectively. The top and the bottom plates which act as condensation and evaporation surfaces are made of brass and both have a thickness of 3 mm and a diameter of 100 mm. 8 bolts were used to fasten the side wall and the top and bottom plates together in order to construct the two-phase thermosyphon. Sealing gaskets were used between the side wall and the top/bottom plates to achieve the sealing requirement. Both the grooved and the un-grooved plates were used for the evaporation and condensation surface. The grooves on the grooved surface are 0.2 mm in width and 1 mm in depth. The grooves radiate from the center of the evaporation surface and the angle between neighboring grooves is 5°, as shown in Fig. 4. The grooved structure can enhance the boiling heat transfer performance of the evaporation surface and besides the micro-grooves can transport liquid from the peripheral region of the evaporation surface to heated region.

Before filling the two-phase thermosyphon, it must be weighed. Then a vacuum pump is used to bring the two-phase thermosyphon to vacuum condition and the working fluid is filled into it. The filling amount is a little bit over the expected value. After that, the two-phase thermosyphon is vacuumized again. But this time, it is heated by hot water during the vacuumizing process in order to extract as much residual air as possible and also to assure the two-phase thermosyphon is full of vapor of the working fluid. At this moment the pressure transducer indicates that the pressure value in the two-phase thermosyphon is 30 Pa. After the weight of the two-phase thermosyphon reaches the expected value, the vacuum valve is closed to keep the vacuum condition. To test its tightness, the two-phase thermosyphon is left in room conditions for 24 hours, and if the pressure of the two-phase thermosyphon as measured by the pressure transducer then is equal to the saturated pressure of the room temperature then we say that the sealing can maintain the vacuum condition for the experimental time. Otherwise the two-phase thermosyphon is brought to vacuum condition again.

3. Results and discussion

3.1. Effect of heating heat flux

Fig. 5 shows the steady-state temperature distributions of the transparent two-phase thermosyphon with the grooved evaporation surface. The working fluid is water and the filling amount of working fluid is 20.5 g. The room air temperature is 19 °C and the velocity of the air that flows on the cooling surface of the two-phase thermosyphon is 9.7 m/s. Due to the small heat transfer coefficient of the side wall and the low thermal conductivity of quartz as compared to brass, the heat dissipated from the sidewall is neglected. The intensity of boiling heat transfer depends on the heat flux if it is lower than the two-phase thermosyphon heat transfer limit. Observation shows that heat transfer on the heated part of the evaporation surface is evaporation when the heating heat flux is small. However, as the heat flux increases, nucleate boiling finally takes place and dominates the phase change heat transfer process.

To study thermal response characteristics of the two-phase thermosyphon, temperature responses are measured in the two-phase thermosyphon, Fig. 6 depicts its temperature responses with a grooved evaporation surface for different heat fluxes. In Figs. 5 and 6, we can see that the time for the spreader to acquire its steady-state decreases with the heating heat flux, but the steady-state temperature of the different positions of the two-phase thermosyphon increases with the heating heat flux. The temperature difference between evaporation and condensation

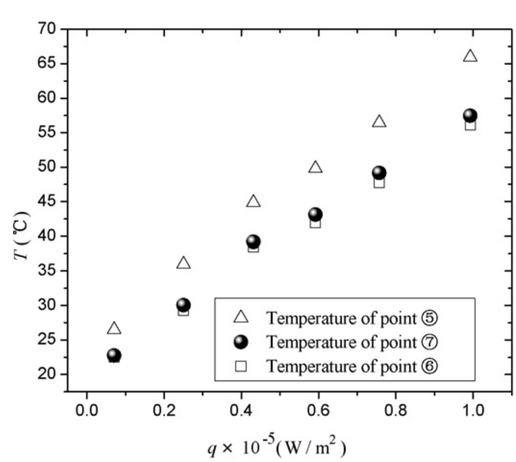

Fig. 5. Steady state temperature of the two-phase thermosyphon with grooved evaporation surface versus heating heat fluxes.

surfaces also increases with the heating heat flux. This is the temperature difference needed to enable boiling and condensation inside the two-phase thermosyphon. Experimental results show that it has a good performance regarding temperature leveling, that is, keeping a uniform temperature distribution on the condensation surface. As we can see, even at the highest heating heat flux within the range of heat fluxes in our experiment, the temperature difference between points ⑥ and ⑦ is only 1.3 °C. We also did experiment with a brass plate that had the same thickness and shape as the two-phase thermosyphon spreader. The results show that the temperature difference between points ⑥ and ⑦ of the brass plate is 6.1 °C for the same heating heat flux. So our experimental results verify the good performance of the two-phase thermosyphon for temperature leveling.

The overall thermal resistance was calculated from the measured temperature difference between the evaporation and condensation surfaces and the heat flux of the heating surface. The results are listed in Table 1. As it is easily understood, smaller thermal resistance means a better performance of the two-phase thermosyphon. From Table 1, we can see that the thermal resistance decreases with the heating heat flux increase, which means that the performance of it improves as the heating heat flux increases. This is due to the fact that boiling and condensation inside the two-phase thermosyphon gradually dominates the process as the heat flux increases, which also indicates that the thermal resistances of the evaporation and condensation surfaces are the main factors that influence the performance of a two-phase thermosyphon.

The startup performance of the two-phase thermosyphon is also recorded. Fig. 6 shows its transient temperature response with a grooved structure for different heating heat fluxes. Fig. 7 presents the transient pressure response inside the two-phase thermosyphon. We observed that during the starting period, the boiling on the evaporation surface becomes increasingly intense

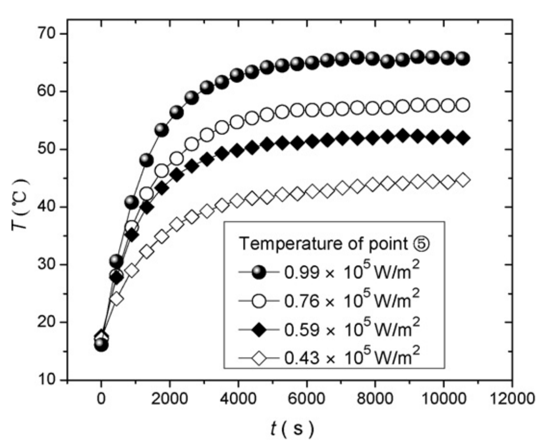

Fig. 6. Temperature responses of the two-phase thermosyphon with grooved evaporation surface.

Table 1
Thermal resistances under different heating heat fluxes

Heating heat flux, 10^5 W/m^2	0.071	0.25	0.43	0.59	0.76	0.99
Thermal resistance, 10^{-4} K m^2/W	5.2	2.4	1.3	1.1	0.96	0.85

as time goes by, and finally a large number of bubbles appear on the central region of the evaporation surface in what is a typical phenomenon of nucleate boiling. In Figs. 6 and 7, it is possible to see that both the temperature and the pressure of the two-phase thermosyphon increase with time. Since the two-phase thermosyphon subjected to vacuum before the working fluid was introduced in it, the working fluid vapor inside it was always in saturated state. During the startup stage, the heating heat flux at the evaporation surface is larger than the cooling heat flux at the condensation surface, and then the temperature and thus the pressure increase with time. After some time, these two heat fluxes become equal and the two-phase thermosyphon reaches its steady state. Its pressure fluctuations are the result of the growth and destruction of the vapor bubbles.

3.2. *Influence of air velocity*

The heat provided by the heating unit is eventually dissipated into the surrounding air by the cooling surface of the top plate. Therefore the heat transfer of the cooling surface should have a very strong effect on the performance of the two-phase thermosyphon. Fig. 8 depicts its steady-state temperature with a grooved evaporation surface and at different air velocities. The air temperature is 19 °C and the working fluid amount is 20.5 g.

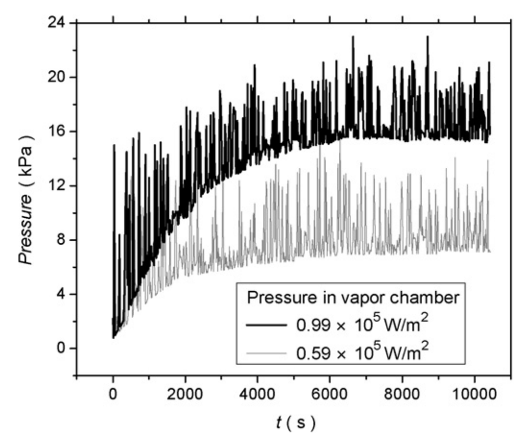

Fig. 7. Pressure response of the two-phase thermosyphon with a grooved evaporation surface.

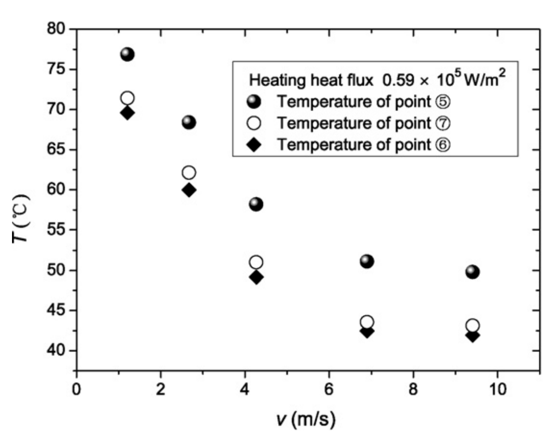

Fig. 8. Influence of air velocity on the steady-state temperature of the two-phase thermosyphon with a grooved evaporation surface.

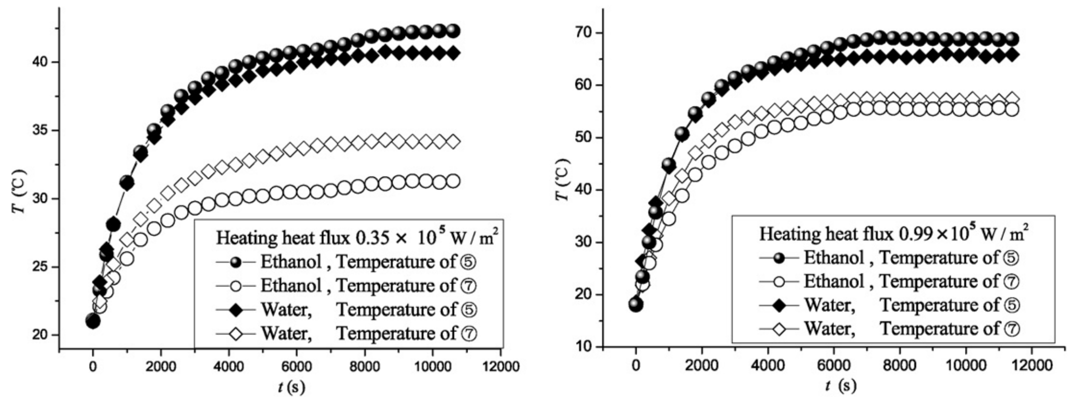

Fig. 9. Temperature responses of the ethanol and water two-phase thermosyphon.

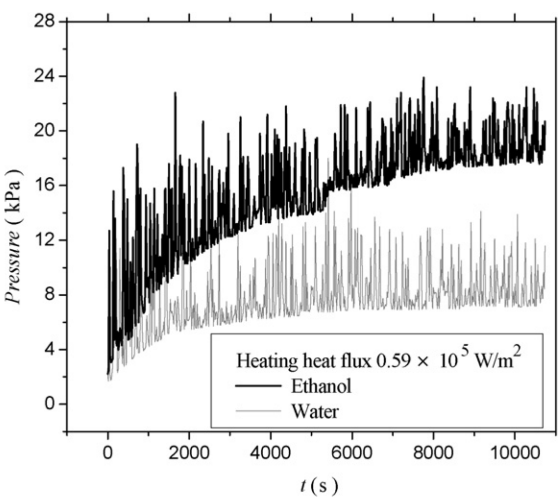

Fig. 10. Transient pressure responses of the ethanol and water two-phase thermosyphon.

The temperature distribution on the condensation surface is not uniform when the air velocity decreases, but the temperature difference between the centers of the evaporation and condensation surfaces is nearly constant except for experimental imprecision. As mentioned earlier, the two-phase thermosyphon is cooled by an impinging air jet. The air velocity therefore reflects the heat transfer intensity on the cooling surface of the top plate, the larger the speed is, the stronger the heat transfer. The improved heat transfer condition on the cooling surface of the top plate causes the temperature of the condensation surface to be lower. This certainly enhances the condensation on the surface.

3.3. Effects of working fluid

In order to investigate the effects of working fluids on the performance of the two-phase thermosyphon, we tested its performances using ethanol and water as the working fluids, respectively. The amount of working fluid is 20.5 g and the air temperature and velocity are all kept at 19 °C and 9.7 m/s respectively. Figs. 9 and 10 show the transient temperature and pressure responses of the two-phase thermosyphon filled with different working fluids and with a grooved evaporation surface. The phase change heat transfer of water is more efficient than that of ethanol. So from Fig. 9, we can see that the temperature difference between the evaporation and condensation surfaces of the ethanol two-phase thermosyphon is larger than that of the water two-phase thermosyphon for the same heating heat flux. This means that the thermal resistance of the ethanol two-phase thermosyphon is larger than that of the water two-phase thermosyphon. Within the range of the tested heating heat fluxes, the performance of the ethanol two-phase thermosyphon is poorer than the one of the water two-phase thermosyphon. The saturation pressure of ethanol is higher than that of water at a given temperature. That is why the pressure of the ethanol two-phase thermosyphon is higher than that of the water two-phase thermosyphon for the same heating heat flux, as shown in Fig. 10.

3.4. The smooth and grooved evaporation surface

Boiling and condensation take place simultaneously inside the two-phase thermosyphon in a narrow space. Therefore its performance depends on the boiling and condensation intensities and on the circulation of the working fluid. A grooved surface is used for the evaporation surface in order to enhance the boiling heat transfer and working fluid circulation.

Fig. 11 shows the boiling phenomenon of the water two-phase thermosyphon with smooth and grooved evaporation surfaces. The experimental conditions are: heating heat flux is $0.76 \times 10^5\ \mathrm{W/m^2}$, air jet velocity is 9.7 m/s and air temperature is 19 °C. From this figure, we can see that the bubbles formed on the grooved surface are smaller in size and larger in number than those on the smooth surface. The bubbles depart more frequently from the grooved surface than from the smooth surface.

Fig. 12 shows the transient temperature response of the two-phase thermosyphon for different surfaces. In this figure, we see that the temperature difference between the evaporation and condensation surfaces of the two-phase thermosyphon with the grooved evaporation surface is generally smaller than that with the smooth evaporation surface. The grooved surface has more boiling nuclei than the smooth surface; hence the bubbles are more easily formed on the grooved surface. This proves that the phase change heat transfer of the grooved surface is greater

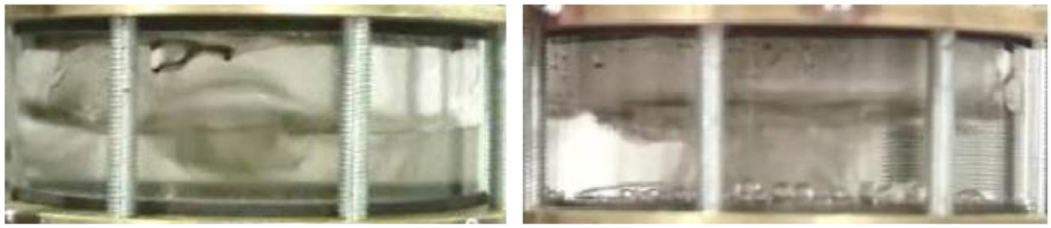

Fig. 11. Comparison of the vapor bubbles formed in the smooth and grooved thermosyphon spreaders.

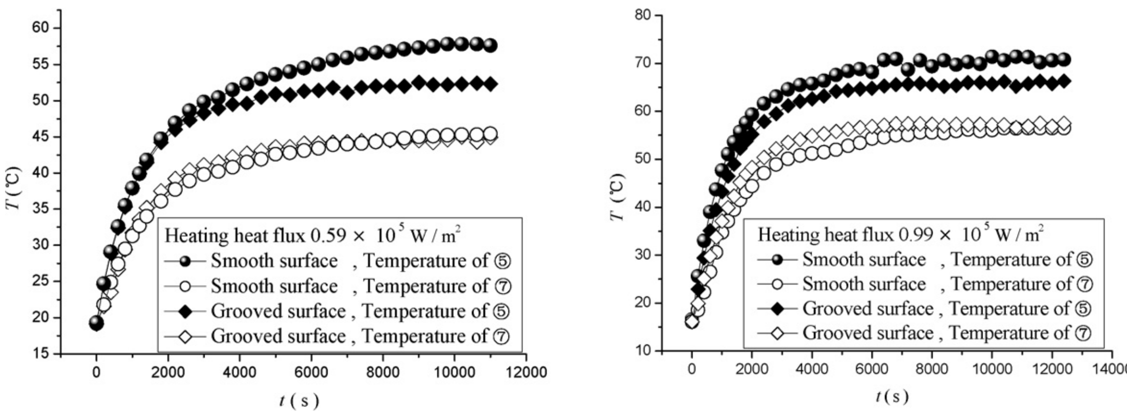

Fig. 12. Temperature responses of the two-phase thermosyphon with different evaporation surfaces.

and working fluid circulation is better. For the steady state, we can see that the temperatures of the condensation surfaces are almost same for these two kinds of two-phase thermosyphons. So if we can increase the phase change heat transfer and decrease the temperature difference between the evaporation and condensation surfaces, the temperature of the heat source will also be smaller at the steady state. This again tells us that ensuring that the working fluid on the evaporation surface at fully boiling state is critical for the two-phase thermosyphon performance and enhancing this boiling heat transfer is the most efficient way to improve it. At higher heat fluxes, the temperature of the evaporation surface of the two-phase thermosyphon with a smooth evaporation surface shows significant fluctuations. This phenomenon results from the fact that the bubbles are large and the departure frequency is small.

4. Analysis of the thermal resistance of the spreader

In order to dissipate more heat from electronic devices into the ambient, heat sinks are generally much larger than heat sources. Due to this, a spreader is usually placed between the heat source and the heat sink to level the heat flux distribution. The traditional spreader is a solid copper plate. But the thermal spreading performance of a solid copper plate deteriorates for increasing heat fluxes and larger base section of the heat sink. Therefore, it is important to study the minimal heat flux beyond which it is necessary to use the two-phase thermosyphon spreader.

The solid copper plate spreader is supposed to be a disk-shaped flat plate and the heat source is under the center of the spreader. The spreading resistance Rs is used to model how heat flows out from a narrow region into a larger cross section region. It can be defined as follows:

$$R_s = \frac{T_{\max} - \overline{T}_{\text{top}}}{Q} \tag{1}$$

Where $T_{\max}$ is the maximal temperature in the spreader which is usually at the center of the plate bottom surface. $\overline{T}_{\text{top}}$ is the average temperature of the spreader top surface. This definition can also be used for the two-phase thermosyphon. Seri Lee and Seaho Song et al. [7,8] used the method of separation of variables to solve the energy equation in a two-dimensional coordinate system. They presented the simple approximation for the dimensional spreading resistance. The dimensional equation can be written as follows.

$$R_s = \frac{\sqrt{A_p} - \sqrt{A_s}}{k\sqrt{\pi A_p A_s}} \times \frac{\lambda k A_p R_0 + \tanh(\lambda t)}{1 + \lambda k A_p R_0 \tanh(\lambda t)} \tag{2}$$

where

$$\lambda = \frac{\pi^{3/2}}{\sqrt{A_P}} + \frac{1}{\sqrt{A_s}} \tag{3}$$

As reported by Song et al., the above correlations agree with the present analytical solutions well within 10% over the range of parameters commonly found in microelectronics applications. Form Eqs. (2) and (3), we can see that the spreading resistance can be determined from the heat source area A_s, plate area A_p, plate thickness t, thermal constriction k and external resistance R_0.

R_0 can be defined as follows:

$$R_0 = \frac{\overline{T}_{\text{top}} - T_r}{Q} \tag{4}$$

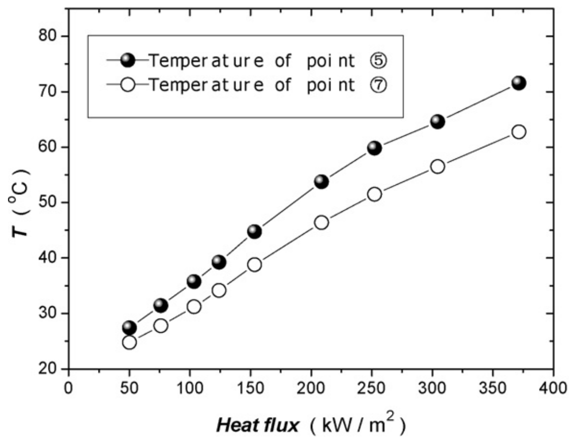

Fig. 13. Steady state temperature of the two-phase thermosyphon.

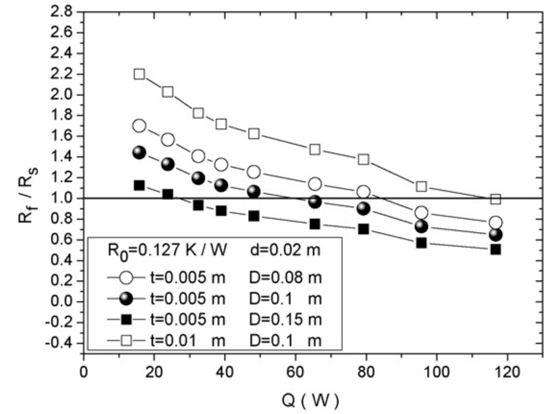

Fig. 14. Spreading resistance ratio of two-phase thermosyphon to solid copper plate.

Where $\overline{T}_{top}$ is the average temperature of the top surface and T_{amb} is the air temperature. In order to obtain the thermal resistance of the grooved two-phase thermosyphon for high heat flux level, we changed the diameter of the heat source to 20 mm and manufactured a new grooved two-phase thermosyphon on the cooling surface of which can be installed a heat sink to improve cooling conditions. Thermocouple positions are the same as the transparent two-phase thermosyphon shown in Fig. 3. Fig. 13 shows the steady state temperature of this new grooved two-phase thermosyphon for a larger range of tested heat fluxes. When we use the same definition with a solid copper plate to calculate the spreading thermal resistance of the two-phase thermosyphon, the average temperature $\overline{T}_{top}$ of the top surface can be replaced by the center temperature T_c of the condensation surface because of temperature uniformity in the condensation surface. Besides, the maximal temperature T_{max} can be replaced by the center temperature of evaporation surface T_e. The spreading resistance of the two-phase thermosyphon can be defined as follow.

$$R_f = \frac{T_{max} - \overline{T}_{top}}{Q} = \frac{T_e - T_c}{Q} \quad (5)$$

So we can use Eqs. (2) and (3) to calculate the thermal spreading resistance of a solid copper plate and compare it to the experimental results for the two-phase thermosyphon. The thermal resistance of the solid copper plate does not change along with the heating heat flux. We are also supposing that the thermal resistance of two-phase thermosyphon does not depend on the thickness within the tested range.

Fig. 14 shows the spreading resistance ratio of the two-phase thermosyphon to the solid copper plate. When the spreading resistance ratios are greater than 1, the two-phase thermosyphon has a worse performance than the solid copper plate. From this figure, we can see that the ratio increases with the thickness and decreases with the heating power and the area of the spreader. So the two-phase thermosyphon should be applied when large base sections of heat sinks and high heating power are involved. For example, if R_0 is 0.127 K/W, d is 0.02 m, t is 0.005 m and D is 0.1 m, the flat plate heat spreader should be applied when the heating power is over 60 W. We know that we can reduce the spreading resistance of a solid copper plate spreader by increasing plate thickness. So the two-phase thermosyphon spreader should be manufactured for small thicknesses, otherwise, it will present worse spreading performance than the solid copper plate in of equal dimensions. In Fig. 14, we can see that when R_0 is 0.127 K/W, d is 0.02 m and D is 0.1 m, if thickness is increased from 0.005 to 0.01 m, the ratio will be greater than 1 throughout the tested range.

5. Conclusions

Transparent two-phase thermosyphons with grooved/ungrooved evaporation surfaces were manufactured as a part of our work for observation study. Thermal behavior and thermal resistance were experimentally studied and the boiling/condensation phenomena were observed. From the experimental results and the above discussions, it is possible to draw the following conclusions: (1) The two-phase thermosyphon shows a very good performance regarding temperature leveling in the condensation surface. (2) Heat transfer on the cooling surface has a very strong influence on the performance of the two-phase thermosyphon. The temperature distribution on the condensation surface is not uniform when the air velocity decreases. (3) Within the range of the tested heat fluxes, the water two-phase thermosyphon has a better performance than the ethanol two-phase thermosyphon. (4) Experimental results prove that the two-phase thermosyphon with a grooved evaporation surface has a much better performance. The grooved surface can increase the boiling heat transfer in the two-phase thermosyphon. (5) The thermal resistances of the evaporation and condensation surfaces are the main factors that influence the two-phase thermosyphon performance; ensuring that the working fluid at the evaporation surface is fully at boiling state is vital to the two-phase thermosyphon; enhancing this boiling heat transfer is the most efficient way to improve its performance. (6) The two-phase thermosyphon should be applied for large base sections of heat sinks and high heating powers. When R_0 is 0.127 K/W, d is 0.02 m, t is 0.005 m and D is 0.1 m, the flat plate heat spreader should be applied when the heating power is over 60 W. And also the two-phase thermosyphon spreader should be manufactured in small thicknesses. When R_0 is 0.127 K/W, d is

0.02 m and D is 0.1 m, if the thickness is increased from 0.005 to 0.01 m, the ratio will greater than 1 for all the tested range.

Acknowledgement

This work is supported by Beijing Education Committee Project No. KM200510005002, Key Lab Project of Beijing University of Technology and Beijing Outstanding Scholar Program (2006).

References

[1] G.E. McCreery, Liquid flow and vapor formation phenomena in a flat heat pipe, Heat Transfer Engrg. 15 (4) (1994) 33–41.
[2] K. Vafai, W. Wang, Analysis of flow and heat transfer characteristics of an asymmetrical flat plate heat pipe, Int. J. Heat Mass Transfer 35 (1992) 2087–2099.
[3] Y. Avenas, C. Gillot, A. Bricard, C. Schaeffer, On the use of flat heat pipe as thermal spreaders in power electronics cooling, in: Power Electronics Specialists Conference, IEEE 33rd Annual 2002, vol. 2, 2002, pp. 753–757.
[4] Y. Avenas, M. Ivanova, N. Popova, C. Schaeffer, J.L. Schanen, Thermal analysis of thermal spreaders used in power electronics cooling, in: Industry Applications Conference, 37th IAS Annual Meeting, vol. 1, 2002, pp. 216–221.
[5] Y. Koito, H. Imura, M. Mochizuki, Y. Saito, S. Torii, Numerical analysis and experimental verification on thermal fluid phenomena in a vapor chamber, Appl. Thermal Engrg. 26 (2006) 1669–1676.
[6] S.-W. Chen, et al., Experimental investigation and visualization on capillary and boiling limits of micro-grooves made by different processes, Sensors Actuators A: Physical 139 (1–2) (2007) 78–87.
[7] S. Song, S. Lee, Van Au, Closed-form equation for thermal constriction/spreading resistances with variable resistance boundary condition, in: Proceedings of the 1994 International Electronics Packaging Conference, Atlanta, GA, 1994, pp. 111–121.
[8] S. Lee, S. Song, Van Au, Constriction/spreading resistance model for electronics packaging, in: ASME/JSME Thermal Engineering Conference, 1995, vol. 4, 1995, pp. 199–206.